

Dynamic X-ray tomography with multiple sources

Esa Niemi, Matti Lassas and Samuli Siltanen

Department of Mathematics and Statistics

University of Helsinki, Finland

Emails: esa.niemi@helsinki.fi, matti.lassas@helsinki.fi, samuli.siltanen@helsinki.fi

Abstract—A novel time-dependent tomographic imaging modality with multiple source-detector pairs in fixed positions is discussed. All detectors record simultaneously time-dependent radiographic data (“X-ray videos”) of a moving object, such as a beating heart. The dynamic two- or three-dimensional structure is reconstructed from projection data using a new computational method. Time is considered as an additional dimension in the problem, and a generalized level set method [Kolehmainen, Lassas, Siltanen, *SIAM J Scientific Computation* 30 (2008)] is applied in the space-time. In this approach, the X-ray attenuation coefficient is modeled by the continuous level set function itself (instead of a constant) inside the domain defined by the level set, and by zero outside. A numerical example with simulated data suggests that the method enforces suitable continuity both spatially and temporally. A drawback of the method is that it is not applicable to real-time imaging.

I. INTRODUCTION

A usual CT measurement setting consists of one X-ray source and one X-ray detector. This setting enables accurate, high-quality reconstructions for a *stationary* body being imaged. However, if the body is moving or changing rapidly, one source-detector pair may not be sufficient to yield useful reconstructions. Modern CT devices are able to measure whole-body data in about one second [4]; thus, any temporal changes in the body that take place in a time interval less than (or approximately equal to) one second are difficult to reconstruct using such devices.

Several CT implementations employing multiple X-ray sources have been proposed. For example, the pioneering Dynamic Spatial Reconstructor of Mayo Clinic [15] makes use of 28 X-ray sources, while dual-source CT devices (using two sources) are also commercially available today [4]. In those implementations, however, the sources are moved during the measurement process, which inevitably means that the fastest possible imaging speed is not attained. To overcome this drawback, we propose a measurement setting consisting of several source-detector pairs in *fixed* positions.

The idea of using fixed sources and detectors is not new: for example, [9], [13], [8], [10], [1] use a ring or array of sources that are pulsed in a specific scanning sequence. However, our approach is different as all the sources radiate all the time. Perhaps the closest study to ours is [16], where the reconstruction method (tomosynthesis) is much simpler than ours.

There are several medical imaging situations where dynamic 3D reconstructions would bring benefits. Examples include cardiac imaging [14] and angiography [16]. In cardiology it

is important to assess the function of the heart over time. However, the duration of a heartbeat is of the order of 1 second, which is difficult to capture using movement-based CT devices. Those difficulties can be mostly overcome using gating, or averaging over several heartbeats, under the assumption that successive heartbeats are (almost) identical.

The benefit of the proposed 4D imaging modality is greater in angiography, where radiopaque contrast agent is injected in the bloodstream. The shape and function of the blood vessels is monitored in the brief time window (again of the order of 1 second) it takes the contrast agent to fill the region of interest and move away. This process can presently be imaged only as radiographic projections, missing 3D information and containing overlaps and geometric distortions. The fixed configuration of multiple source-detector pairs enables following the movement of the contrast agent in a time-dependent and three-dimensional fashion.

Other end users of the proposed technique can be found in veterinary medicine and biological laboratories [12]. Four-dimensional small animal imaging would allow unprecedented studies of anatomy and physiology of naturally moving animals.

The difficulty in the proposed fixed-source setting is that, due to practical reasons, the number of projection images available at one instant of time is small (e.g. less than 20). This makes traditional reconstruction algorithms such as filtered backprojection suboptimal in the resulting *ill-posed* reconstruction task. To overcome the difficulty, we propose a computational method making use of the following two assumptions:

- A1 the body moves/changes slowly with respect to the detectors’ imaging frequency, and
- A2 the attenuation coefficient is nonnegative, i.e. X-ray intensity does not increase inside the body.

The approach is based on the ideas and results in [6], with its motivation coming from level set methods and generalized Tikhonov regularization.

Earlier sparse tomography algorithms, dealing with similar data than here, can be found in [2], [3], [5]. A more comprehensive list of references is given in [11, Chapter 9].

This paper is organized as follows. In Section 2 we describe the fixed multi-source measurement setting and discuss briefly its features. Section 3 introduces the computational reconstruction method, and in Section 4 we present a numerical example to illustrate how the proposed method handles the problem of

strongly limited projection data in the dynamic CT setting. Finally, Section 5 draws conclusions.

II. MEASUREMENT SETTING OF FIXED SOURCES

To avoid the time-taking rotations and other movements in the CT measurement system, we consider a setup consisting of several fixed source-detector pairs, see Figure 1 for an illustration. We assume that all the detector-source pairs take projection images simultaneously. This means that at each instant of time, a whole set of projection images is measured. The temporal resolution of this setting is restricted only by the imaging speed of the X-ray detectors; modern X-ray detectors can take up to 88 frames per second, yielding an effective scan time of 11ms.

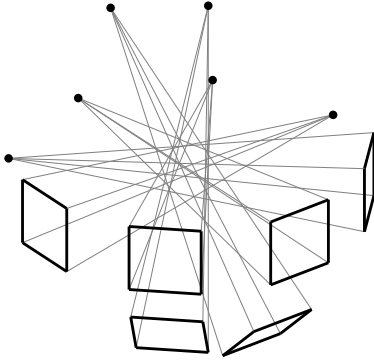


Fig. 1. Example of a measurement setup with six x-ray sources and six detectors in three spatial dimensions. The sources are denoted by dots and the detectors by bold square-shaped frames.

In the sequel, we consider the resulting dynamic CT problem only in two spatial dimensions, despite the fact that the methods and ideas can be readily extended to three dimensions. An example of a two dimensional measurement setting in fan-beam geometry with nine sources and nine detectors is shown in Figure 2.

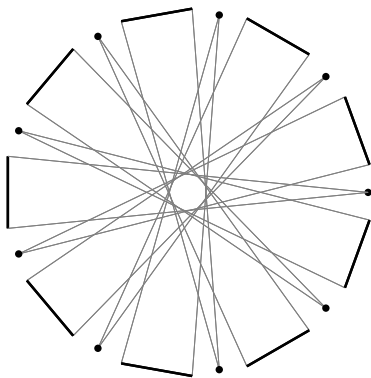


Fig. 2. Example of a measurement setup with nine x-ray sources and nine detectors in two spatial dimensions. The sources are denoted by dots and the detectors by bold lines.

III. RECONSTRUCTION METHODS

In this section we introduce the new computational method for computing dynamic CT reconstructions in two spatial dimensions. In order to have a benchmark algorithm for the new method, we consider the “corresponding” generalized Tikhonov regularization method that makes no use of assumptions A1 or A2 but computes the reconstructions separately at each instant of time.

A. Proposed level set method type regularization

To formulate the inverse problem of dynamic 2-D X-ray tomography considered in this study, let us model the direct problem at an individual time instant t by

$$m_t = \tilde{A}v_t + \varepsilon_t, \quad (1)$$

where m_t denotes the measurement data (sinogram) obtained at time t , \tilde{A} is a linear operator mapping each object $v_t = v_t(x, y)$, $(x, y) \in \Omega \subset \mathbb{R}^2$, to the corresponding measurement m_t , and ε_t denotes the errors in the measurement. In this model the operator \tilde{A} can be considered as the standard 2-D Radon/x-ray transform. Note that it does not depend on time.

Now, the idea is to consider the dynamic problem as a stack of the above problems in 3-D space by taking time t as the third variable, see Figure 3 for an illustration. Analogously, we can stack the set of problems (1) for k consecutive instances $t = 1, 2, \dots, k$ to get the final model

$$m = Av + \varepsilon. \quad (2)$$

Here, with vector notation, $m = [m_1, m_2, \dots, m_k]^T$, and A , v and ε are defined correspondingly.

The inverse problem we consider is: given m and A , determine $v = v(x, y, t)$. We propose to solve this problem using an adapted version of the method introduced in [6]. More precisely, we find the solution in the form

$$f(\Phi(x, y, t)), \quad (3)$$

where $f: \mathbb{R} \rightarrow \mathbb{R}$ is given by

$$f(z) = \begin{cases} z, & \text{if } z \geq 0 \\ 0, & \text{if } z < 0 \end{cases}$$

and $\Phi(x, y, t) := \lim_{s \rightarrow \infty} \phi(x, y, t, s)$ is sought as the solution of the evolution equation

$$\begin{cases} \phi_s = -A^*(A(f(\phi)) - m) + \beta\Delta\phi \\ (\nu \cdot \nabla - r)\phi|_{\partial\Omega} = 0 \end{cases} \quad (4)$$

with a suitable initial condition $\phi(x, y, t, 0) = \phi_0(x, y, t)$. Here $\beta > 0$ is a regularization parameter, $r \geq 0$, A^* denotes the transpose of A , and the Laplace operator includes derivatives in t , that is $\Delta\phi = \phi_{xx} + \phi_{yy} + \phi_{tt}$.

This approach can be seen as a generalization of level set methods ([6]) with the evolution equation based on minimizing the slightly modified generalized Tikhonov functional,

$$\arg \min_u \{ \|Af(u) - m\|_2^2 + \beta \|\nabla u\|_2^2 \}, \quad (5)$$

where $|\cdot|$ denotes the standard Euclidean norm. Compared to classical level set methods, we use f instead of the Heaviside

function in (3) and (4). This means that, inside the level set, we represent the attenuation coefficient by the level set function itself (not by a constant). On the other hand, f is smoother than the Heaviside function, which makes analysis of (4) easier. The trick in (5) is to use $f(u)$ instead of u in the discrepancy term.

Note that the representation (3) ensures that the solution be nonnegative, while the Laplace term $\beta\Delta\phi$ in (4) enforces continuity (of the solution) not only in spatial but also in temporal direction. Thus assumptions A1 and A2 are taken into account in the method.

Computationally the essential part of the method is solving the evolution equation (4). We use the classical Euler's method for this.

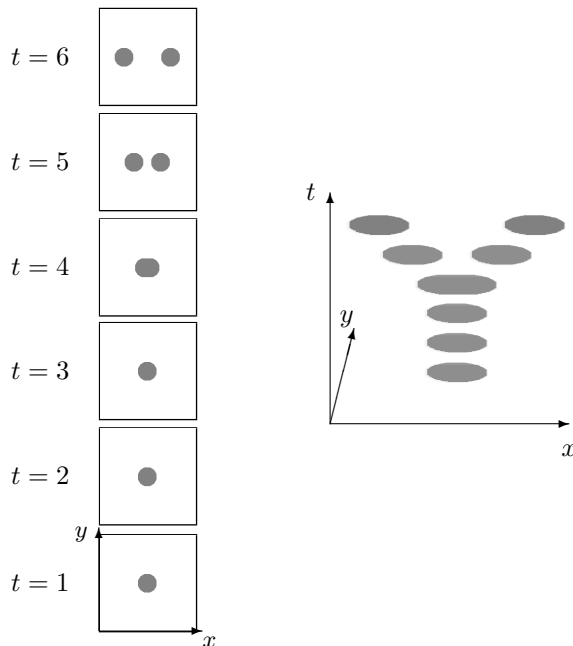


Fig. 3. Illustration of the idea in 2+1-dimensional spatio-temporal interpretation. Left: six states $v_t = v_t(x, y)$ of a dynamic 2-D object at $t = 1, \dots, 6$. Right: the same dynamic object considered in three-dimensional Euclidean (x, y, t) -space as $v = v(x, y, t)$.

B. Generalized Tikhonov regularization

Next we consider a standard version of the generalized Tikhonov regularization. For this method it is sufficient to consider problem (1), that is, given the measurements m_1, m_2, \dots, m_k , we simply solve the corresponding equations (1) separately for each m_j by finding the minimizers

$$\arg \min_u \left\{ \|\tilde{A}u - m_j\|_2^2 + \alpha \|\nabla u\|_2^2 \right\}, \quad (6)$$

where $j = 1, \dots, k$ and $\alpha > 0$ is a regularization parameter. The minimizers can be found numerically using some iterative optimization method; we use a preconditioned conjugate-gradient algorithm.

IV. NUMERICAL EXAMPLE

We present a numerical example to illustrate the performance of the proposed method in a measurement setting with

nine (9) sources as demonstrated in Figure 2. We compare the proposed method to generalized Tikhonov regularized solutions computed separately at each time step. Details on these methods are explained in Section III. The test data was simulated for a similar “Y-shaped” object as shown in Figure 3 (here with finer resolution, though). After the simulation, 5% Gaussian white noise was added to the data.

The evolution equation (4) was solved numerically using Euler's method with 50 steps ending at $s = 1000$ and with initial state $\phi_0 \equiv 0$. The spatio-temporal (x, y, t) -resolution in the example is $100 \times 100 \times 100$. The regularization parameters are $\beta = 3 \cdot 10^{-3}$ for the proposed method and $\alpha = 10^{-2}$ for the generalized Tikhonov method; they were chosen by trial and error such that the relative L^2 errors of the reconstructions were approximately minimized. The Laplace operator was discretized using central difference approximations with a unit spacing in all x, y and t directions and assuming Neumann boundary condition on the boundary (i.e. $r = 0$). The reconstructions for three different stages with relative L^2 errors are shown in Figure 4. In addition, an isosurface plot of the reconstruction computed by the proposed method is shown in Figure 5.

There was no big difference in the computation times of the two methods. The main computational cost comes from projections and back-projections, and the number of those is of the same order of magnitude in both methods.

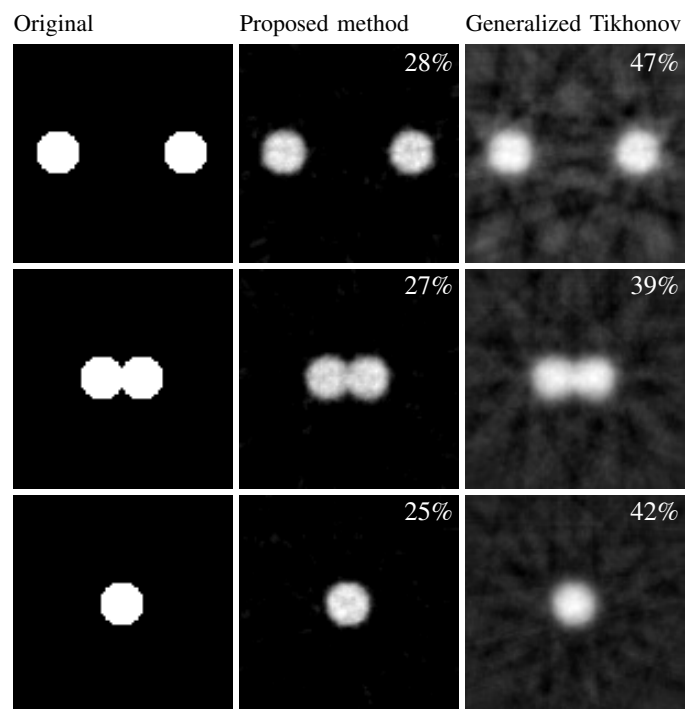


Fig. 4. Reconstructions of the Y-shaped object at three different stages. The relative L^2 errors are shown in the upper right corners of the reconstructions.

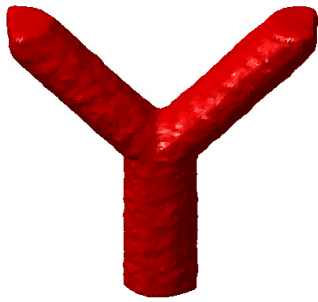


Fig. 5. Isosurface plot of the Y-shaped object reconstructed by the proposed computational method. The axes here are the same as those on the right-hand side of Figure 3.

V. CONCLUSION

Dynamic X-ray tomography with multiple fixed source-detector pairs enables high temporal resolution but leads to sparse set of projection data. To obtain useful reconstructions from such a sparse data set, advanced reconstruction algorithm might be necessary. The proposed computational method seems to combine suitable regularization both spatially and temporally; compared to the rather standard generalized Tikhonov regularization, it produces reconstructions with smaller L^2 errors and closer to the original object as judged by visual inspection as well.

A drawback of the proposed reconstruction algorithm is that it is not applicable to real-time imaging because all the projection data at all time steps is needed before computing the reconstructions. On the other hand, there is an open question, how to optimally choose the regularization parameter β , or the ending point and step size of the Euler scheme. Also, the spacing (or scaling) in t -direction can be chosen freely, independent of the spatial spacings in x and y directions; it might, however, have a significant effect on the reconstructions.

This pilot study contains only simulated data, and the true value of the proposed method can be seen only after real data experiments. There are several challenges:

- Geometric restrictions arising from the closeby arrangement of multiple sources and detectors: multiple cone beams can probably cover only a relatively small volume.
- The intensity of the sources needs to be rather high to ensure reasonable signal-to-noise ratio in the short time frames of the X-ray videos.

To conclude, the proposed method seems to have promise for 4D medical and biological imaging, but only further studies will reveal how useful it is in practice.

ACKNOWLEDGMENT

This work was supported by the Academy of Finland (project 141094 and Finnish Centre of Excellence in Inverse

Problems Research, decision number 250215).

REFERENCES

- [1] D. Bharkhada, H. Yu, H. Liu, R. Plemmons, and G. Wang, *Line-Source Based X-Ray Tomography*, International Journal of Biomedical Imaging Volume 2009.
- [2] G. T. HERMAN AND A. KUBA, *Discrete Tomography: Foundations, Algorithms, and Applications*, Birkäuser, 1999.
- [3] Herman, G. T. and Kuba, A. (2003). Discrete tomography in medical imaging. *Proceedings of the IEEE*, 91(10), 1612-1626.
- [4] W. A. Kalender, *X-ray computed tomography*, Physics in Medicine and Biology **51**, R29-R43, 2006.
- [5] V. KOLEHMAINEN, S. SILTANEN, S. JÄRVENPÄÄ, J. KAPIO, P. KOISTINEN, M. LASSAS, J. PIRTTILÄ, AND E. SOMERSALO, *Statistical inversion for medical X-ray tomography with few radiographs: II. application to dental radiology*, Physics in Medicine and Biology, 48 (2003), pp. 1465-1490.
- [6] V. Kolehmainen, M. Lassas and S. Siltanen, *Limited data X-ray tomography using nonlinear evolution equations*, SIAM Journal of Scientific Computation **30**(3), pp. 1413-1429, 2008.
- [7] Y. Liu, H. Liu, Y. Wang and G. Wang, *Half-scan cone-beam CT fluoroscopy with multiple x-ray sources*, Medical Physics, Vol. **28**, No. 7, 2001.
- [8] S. R. Mazin, J. Star-Lack, N. R. Bennett and N.J. Pelc: *Inverse-geometry volumetric CT system with multiple detector arrays for wide field-of-view imaging*, Medical Physics 34(6), 2007, pp. 2133-2142.
- [9] E. J. Morton, R. D. Luggar, M. J. Key, A. Kundu, L. M. N. Tavora, and W. B. Gilboy, *Development of a high speed x-ray tomography system for multiphase flow imaging*, IEEE Trans. Nucl. Sci., vol. 46 III(1), pp. 380384, 1999.
- [10] E. Morton, K. Mann, A. Berman, M. Knaup, and M. Kachelriess, *Ultrafast 3D reconstruction for x-ray real-time tomography (RTT)*, in Nuclear Science Symposium Conference Record (NSS/MIC), 2009 IEEE, Nov 2009, pp. 40774080.
- [11] J. MUELLER AND S. SILTANEN, *Linear and Nonlinear Inverse Problems with Practical Applications*, SIAM, 2012.
- [12] M. J. Paulus, S. S. Gleason, S. J. Kennel, P. R. Hunsicker and D. K. Johnson, *High resolution X-ray computed tomography: an emerging tool for small animal cancer research*, Neoplasia, Vol. **2**, pp. 62-70, 2000.
- [13] E. Quan and D. S. Lalush: *Resolution Effects in a Dense Linear Source Array X-ray Micro-tomograph*, in 2005 IEEE Nuclear Science Symposium Conference Record M07-185, pp. 2094-2097.
- [14] E. L. Ritman, *Cardiac computed tomography imaging: a history and some future possibilities*, Cardiology Clinics **21**, pp. 491-513, 2003.
- [15] R. A. Robb, E. A. Hoffman, L. J. Sinak, L. D. Harris and E. L. Ritman, *High-speed three-dimensional X-ray computed tomography: the dynamic spatial reconstructor*, Proceedings of the IEEE, Vol. **71**, No. 3, pp. 308-319, 1983.
- [16] G. M. Stiel, L. S. G. Stiel, E. Klotz and C. A. Nienaber, *Digital flashing tomosynthesis: a promising technique for angiographic screening*, IEEE Transactions on Medical Imaging 12(2) 1993, pp. 314-321.